Shielded open-circuited probe for in-situ measurements of soil permittivity in Very high frequency (VHF) and Ultra high frequency (UHF) bands

Konstantin Muzalevskiy and Andrey Karavaysky

Abstract

In this paper, the shielded open-circuited probe operating in the wide frequency range from 75MHz to 2GHz is proposed. The probe is made of an SubMiniature version A (SMA) flange connector. The central rod of the SMA connector emerges from a coaxial transition in the flange and shielded by four rods. The robe design allows us to calculate of the probe reflection coefficient S_{11} used simple analytical transmission line model (TEM wave mode), the parameters of which were calibrated on a set of substances with a known frequency spectrum of permittivity. The refractive index (RI) and normalized attenuation coefficient (NAC) retrieval technique is based on solving the inverse problem of minimizing the residual norm between measured and calculated frequency spectra of reflection coefficient S_{11}. After calibration, the root-mean-square error (determination coefficient) between the measured and calculated module and phase of the reflection coefficient S_{11} for the sets of calibration media air, distilled water, butanol, pure ice, water solution with NaCl of salinity of 8.9% do not exceed 0.26dB (0.995) and 0.03 rad (0.999), respectively, in the frequency range from 75MHz to 2GHz. The root-mean-square error (determination coefficient) between the measured RI and NAC spectra for four soil cover samples (variation of the clay fraction from 10.5 g/g to 47.6 g/g) using the proposed probe and a precision coaxial cell not exceeds 0.109 (0.993) and 0.057 (0.986), respectively, in the frequency range from 75 MHz to 2 GHz. As a result, it is experimentally shown that RI и NAC can be measured by the proposed non-precision probe with an error comparable to the precision coaxial cell.

Keywords

Soil measurements, dielectric spectroscopy, frequency domain reflectometry, complex permittivity, shielded open-circuited probe

Introduction

Information on complex permittivity (CP) and its depth distribution in the active layer is critical for improving the calibration accuracy of space radars and radiometers, solving direct problems of microwave emission and scattering, retrieving soil moisture and temperature, developing methods for determining the frozen or thawed states of the topsoil based on remote sensing data in P- and L-bands (Du et al., 2015).

Commercially available reflectometric dielectric tools (Jackisch et al., 2020) are frequency limited. For example, ThetaProbe ML2x is an impedance reflectometer working on a frequency of 100 MHz (Bircher at al., 2016; Jackisch et al., 2020), or TRIME-PICO is a time-domain reflectometer (TDR) that measures only an apparent refractive index at a frequency of about 2.5GHz, which corresponds to the group velocity of impulse that propagates in waveguide line, placed into the soil (Jackisch et al., 2020). The measured soil volume by these sensors is quite large (about 300–1500 cm³), that prevents the detailed study of the fine structure of the CP profiles in active topsoil during its natural moistening and drying or in the case as the front of freezing and thawing moves in the soil (Lemmetyinen et al., 2016) . Currently developed TDR/FDR methods for measuring CP spectrum of soil have a significant error in L-band at frequencies above 0.5-1.0 GHz (Lin at al., 2017; Szyplowska et al., 2015).

Recently, a number of broadband open-ended coaxial sensors have been proposed, which are either completely inserts into the soil (Lin at al., 2017; Majcher et al., 2020; Szerement et al., 2019, 2020; Szyplowska et al., 2015; Wilczek et al., 2016; Woszczyk et al., 2020, 2019), or it touches of soil surface without penetration in it (Demontoux et al., 2017; Guihard et al., 2020, 2019; Mavrovic et al., 2018, 2020, 2021). The CP measuring method based on an open-ended flange coaxial probe (Demontoux et al., 2017; Komarov et al., 2016)

Kirensky Institute of Physics Federal Research Center KSC Siberian Branch Russian Academy of Sciences, Russian Federation

Corresponding author:
Konstantin Muzalevskiy, Kirensky Institute of Physics Federal Research Center KSC Siberian Branch Russian Academy of Sciences, Akademgorodok 50/38, Krasnoyarsk, 660036, Russian Federation.
Email: rsdkm@ksc.krasn.ru

is primarily used for homogeneous liquid and semi-liquid materials for which a good contact between the medium and flange is provided. At the same time, due to the small contact area of the open-ended flange probe with the soil surface, poor repeatability of measuring CP values for natural soils in the field conditions is achieved. Shielded open-ended coaxial-waveguide probes (Lin et al., 2017) prevent natural fluxes of moisture and heat in the soil through the probe's measuring area. The main limitation of existing shielded open-ended coaxial-waveguide probes spectroscopic methods of measuring CP is the incapability of their application directly in the soil due to the design of shielded open-circuited (Lin et al., 2017) or closed cylindrical (Baker-Jarvis et al., 2004) coaxial cells that prevent natural fluxes of moisture and heat in the soil through the measuring area of probes. Probe in fork-shaped configuration, which is consisting of one central and several shielding rods, is the most suitable for measuring ultrabroad band spectrum of soil permittivity (Heimovaara, 1994, 1996; Lin at al., 2017; Majcher et al., 2020; Szerement et al., 2020, 2019; Szyplowska et al., 2015; Wagner, 2011; Woszczyk et al., 2020, 2019; Xu et al., 2012). The use of a large number of densely placed shielding rods (six and more) makes it possible to minimize the wavefield distortion of the main Transverse electromagnetic (TEM) mode. Therefore a simple transmission line model can be used to calculate electromagnetic field distribution in the waveguide section (Heimovaara, 1994, 1996; Lin at al., 2017; Robinson et al., 2003; Wagner, 2011; Xu et al., 2012). However, at frequencies more than 500 MHz-1GHz, the error of permittivity measurements used fork-shaped sensors is still high (Heimovaara, 1994, 1996; Szerement et al., 2020, 2019; Szyplowska et al., 2015; Woszczyk et al., 2020, 2019; Xu et al., 2012). In this frequency range, the design of existing fork-shaped sensors allows the formation of higher wave modes with respect to the principal TEM, which will not be possible to use simple retrievals models (Heimovaara, 1994; Lin at al., 2017; Robinson et al., 2003; Wagner, 2011; Xu et al., 2012) to reconstruct the CP spectra above 0.5-1 GHz with the required accuracy. The use of numerical methods, such as finite element method (FEM), allows to build an accurate electrodynamic model and accurately calculate the field of the wave in a non-precision coaxial line mounted on two N-type connectors shielded by four rods (Wagner, 2011). As a result, based on a numerical solution, it is possible to measure the permittivity spectrum of the soil in a wide frequency range from 1 MHz to 10 GHz (Wagner, 2011). In Wilczek et al. (2016), contrasting with Wagner (2011), a shielded open-circuited probe with four shielding rods was designed based on the N-type connector. The authors proposed a method that enables selective determination of dielectric relaxation time and electrical conductivity of a material using the amplitudes of two TDR pulses widths of 300ps and 800ps (Wilczek et al., 2016). As in Wagner (2011), this method was based on numerical (Finite difference time domain – FDTD) calculation of S_{11} parameter, take into account a real geometry of the probe. Moreover, measuring the CP spectrum in a wide frequency range was not formulated (Wilczek et al., 2016). In further studies (Szerement et al., 2019, 2020), the authors, based on the approaches of Wagner (2011) of complete numerical electrodynamic simulation of the shielded open-circuited probe,
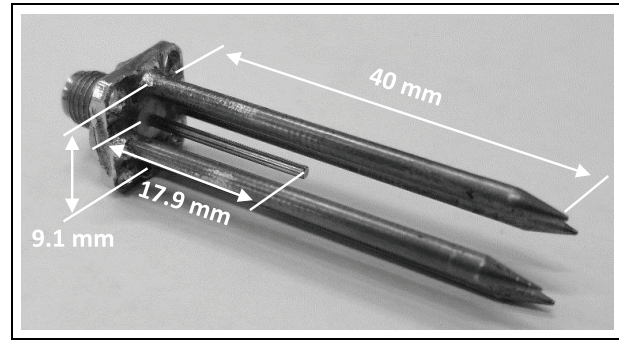

Figure 1. The dielectric probe, manufactured based on an SMA flange.

proposed a method for measuring CP spectra up to 200-500 MHz. In the last works of Woszczyk et al. (2020, 2019), a constructed in form of a monopole open-ended insulated probe allows measuring CP in the frequency range from 50 MHz to 350 MHz.

The main idea of our work is to modify the proposed constructions of non-precision coaxial probes (Szerement et al., 2019, 2020; Wagner, 2011; Wilczek et al., 2016) in order to extend the frequency range of soil CP measurements. The proposed design of a non-precision shielded open-circuited probe, in contrast with the approaches of Szerement et al. (2019, 2020), Wagner (2011), Wilczek et al. (2016), Woszczyk et al. (2020, 2019), allows the use of an analytical simple coaxial transmission line model to reconstruct CP spectra, rather than to use a direct numerical electrodynamic model (FEM, FDTD) of the probe. In contrast with Lin at al. (2017), the proposed design of a non-precision shielded open-circuited probe is easier to manufacture and provides natural fluxes of moisture and heat through the measuring probe's area.

Measuring system and probe

To ensure the natural migration of moisture and heat fluxes through the measuring area of the probe, the outer shell of the probe was constructed of four shielding rods similarly as in Wagner (2011), Wilczek et al. (2016) and Szerement et al. (2019, 2020). The probe's view, which was mounted on an SubMiniature version A (SMA) flange, is shown in Figure 1.

The length and diameter of the central rod are equal to $l_p = 17.9$ mm and $a = 1.27$ mm, respectively (from flange). The length and diameter of the outer four rods are equal to 40.0 mm and 2.4 mm, respectively. The centres of the outer cylindrical rods are located on a circle with a diameter of $b = 9.1$ mm. In CST Microwave Studio, the probe was modelled in real geometry, shown in Figure 1. The SMA connector was excited using a waveguide port through a simulated coaxial cable with an impedance of 50 Ohm and a length of 10 cm, whose cross-section coincided with SMA connector ones. (Note that this simulation did not take into account the transition of N-type to SMA-type adapter that was used in the experiment to connect the cable of vector network analyzer (VNA) with the SMA-probe). The reflection coefficient S_{11} was calculated based on the FDTD method for a set of parameters: the position of shielding rods with respect to the

Table 1. Soil texture (by weight), moisture content and dry bulk density of soil samples [*].

| | Number of soil samples | | | |
	1	2	3	4
Moisture [cm^3/cm^3]	27.6	33.9	46.5	45.1
Sand [%]	41.4	40.4	1.6	45.1
Silt [%]	48.1	40.3	66.2	50.4
Clay [%]	10.5	19.4	32.2	47.6
ρ_d^{probe} [g/cm^3]	1.701	1.712	1.436	1.200
ρ_d^{cell} [g/cm^3]	1.780	1.740	1.377	1.386

[*] ρ_d^{probe} and ρ_d^{cell} is the soil bulk dry density of soil samples in plastic cups and coaxial cells, respectively.

center conductor and their number, the length of the shielding rods relative to the length of the center conductor. The simulation showed that with increasing the number of shielding rods from 4 to 6, the calculation accuracy of frequency spectrum S_{11} practically does not increase. At this, the volume distribution of the field inside the probe practically does not extend in the longitudinal direction beyond the cross-section of the probe near at the end of the centre rod. Next, the optimal distance for placement of the shielding rods relative to the central rod was adjusted, for the configuration of which a simple transmission line model (TEM mode) in the frequency range from 75 MHz to 2 GHz can be used to calculate the reflection coefficient S_{11} for air, butanol, distilled water with the root-mean-square error (RMSE) less than 1.0dB. Experimental testing of the constructed probe was performed under laboratory conditions at an air temperature of 21°C with using four soil samples, moistened with distilled water and placed in plastic cups of volume 100 ml. The soil samples were selected from the mineral horizon of Arctic soils in the Yamal Peninsula and in the central part of Russia, texture and volumetric moisture of which are given in Table 1.

The probe through the N to SMA connector and the high-precision coaxial test cable was connected to the VNA Agilent FieldFox 9927A to measure the complex reflection coefficient S_{11}. Before measurements, calibration of VNA was performed by standard mechanical calkit (Full 2-port Cal, 85518A, Type-N-50Ohm) after a 30-minute warm-up time. VNA has a measurement uncertainty on average 0.35dB for magnitude and 1.9° for the phase in the range of reflection magnitude from -20 to 0dB and at frequencies <9GHz. The S_{11} parameter was measured in the frequency range from 75 MHz to 6 GHz when the probe was placed in four different locations of the soil specimen (see Figure 2). In this case, to average the influence of density and reduce the effect of air gaps in soil samples in each case, three measurements were carried out at a vertical displacement of the probe deep into the soil by ˜ 1 mm. At the same time, the refractive index and the attenuation coefficient of these soil samples were measured with the use of a precision coaxial cell and technique described in (Mironov at al., 2017). The cylindrical cell formed by a section of the precision coaxial waveguide with a cross-section of 7/3 mm. The length of the sample placed in the cell and its volume were equal to 17 mm and 0.529 cm^3, respectively. The four

Figure 2. The process of measuring CP spectrums by the probe placed into plastic cap using VNA.

soil samples were moistened to varying degrees, mixed well and stored in four sealed containers at least for one day.

Then, the soil sample was taken from one of the containers and divided into three parts. The first part of the soil was used for moisture measuring, using a thermostat-weight method (during 4–6 hours). The remaining two parts of the soils were sent to a coaxial cell and a plastic cup. Soil samples in a coaxial cell and a plastic cup were compacted with a small metal cylindrical and ceramic pestle to remove air gaps and have a similar density. As a result, it was possible to achieve close values of the soils samples density in the coaxial cell and in the plastic cup (see Table 1).

Transmission line model and inverse method

The probe may be considered as a coaxial transmission line section (sample holder section) terminated by an open circuit, which propagates only in TEM mode (Baker-Jarvis et al., 2004; Bussey, 1980). Wave impedance, Z_s, of the section with an effective length of l_s can be represented in the form

$$Z_s = \frac{Z_{s0}}{\sqrt{\varepsilon_s}} \frac{1 + exp(2ik_0\sqrt{\varepsilon_s}l_s)}{1 - exp(2ik_0\sqrt{\varepsilon_s}l_s)} \quad (1)$$

where $Z_{s0} = 138 \cdot lg(b_e/a)$, b_e is an effective diameter of the outer shell (constructed with four shielding rods); $k_0 = 2\pi f/c$ is a wavenumber of free space, f is a frequency of microwave, c is the speed of light in vacuum; $\varepsilon_s = \varepsilon_s(f)$ is CP of the sample. In (1) it is assumed that the TEM wave reflects from some
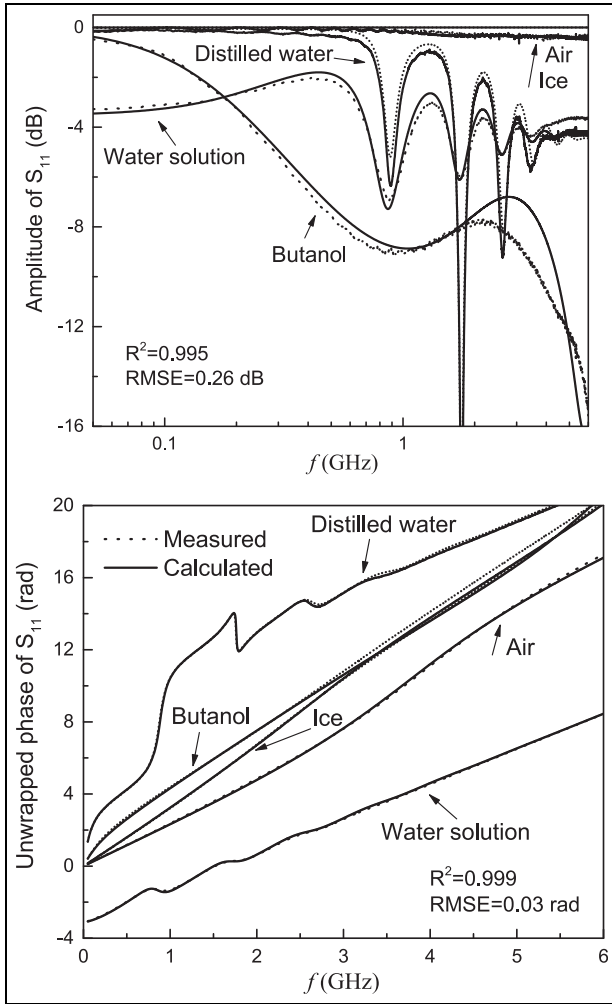
Figure 3. Amplitude and unwrapped phase of reflection coefficient S_{11} for different calibration environments.
Statistical estimates were obtained in the frequency range from 75 MHz to 2 GHz.

plane in cross-section of the probe, placed at a distance of $l_s > l_p$, with a reflection coefficient equal to 1. The higher modes at the discontinuity are modelled as a correction in length, l_s, due to the fringing capacitance at the end of the inner conductor (Baker-Jarvis et al., 2004). The reflection coefficient, S_{11}, of the TEM wave from the probe (at the end of the coaxial cable of VNA in calibration plane of N-connector) can be represented in the form

$$S_{11} = \frac{Z_s - Z_c}{Z_s + Z_c} exp(2ik_0 l_c) \qquad (2)$$

Here, Z_c is an effective impedance, and l_c is an effective length of transmission line from the calibration plane of the N-connector to the flange of the SMA connector. Adjust the parameters b_e, Z_c and l_c allow to simplified take into account the mismatch of the characteristics of waveguide lines between calibration plane of N-connector at the end of the coaxial cable of VNA and flange of the SMA connector, when

propagating between them the wave additionally attenuates and having phase shifts. Based on the model (1)–(2), the reflection coefficient S_{11} for a given CP of the specimen is a function of the following variables: $\vec{p} = (b_e, l_s, Z_c, l_c)$, which need to be calibrated. These parameters will be assumed as effective constant values for the entire frequency range, then only one measurement of the frequency spectrum of S_{11} is needed to determine them. Let us estimate the error of determining the parameters $\vec{p}$ depending on a different set of calibration substances. The mean values and the standard deviations, $\Delta \vec{p}_0$, of the parameters $\vec{p}_0 = (7.58 \pm 0.18$ mm, 19.44 ± 0.29 mm, 49.59 ± 0.12 Ohm, 46.36 ± 0.44 mm) were found during calibration using as calibration standards following substances with known permittivities: air ($\varepsilon_s = 1.0$), a water solution of *NaCl* with a salinity of 8.9% (Stogryn, 1971), distilled water (Stogryn, 1971), ice ($\varepsilon_s = 3.15 + i \cdot 0$), and butanol (Buckley et al., 1958). In this case, the minimizing problem of residual norm between the measured and calculated values of the spectrum of reflection coefficients S_{11} in the frequency range from 75 MHz to 6 GHz was solved (at this purpose, all possible combinations of the residual norms were calculated for various sets of calibration substances). The value of $\Delta \vec{p}_0$, obtained for the parameters, $\vec{p}_0$, are used below to estimate the error for indirect measurements of the soil CP using the probe (see (4)). As an example in Figure 3, the results of comparing the measured and calculated S_{11} (with the optimally found parameters $\vec{p}_0$ during calibration) are shown.

From Figure 3, it can be seen that model (1)–(2) with optimally found parameters $\vec{p}_0$ with a high correlation coefficient (R^2) and a low RMSE describes the experimental values of the reflection coefficient for different calibration substances. At the same time, due to the simplicity of the model (1)–(2), the calibration error increases in the frequency range above 2 GHz (see Figure 3). The obtained estimates of the parameters, $\vec{p}$, for the simplified sets of calibration media: air and water solution of NaCl, $\vec{p}_1 = (7.48$ mm, 19.7 mm, 49.5 Ohm, 45.9 mm), only air, $\vec{p}_2 = (7.602$ mm, 18.9 mm, 49.66 Ohm, 47.1 mm), are in good agreement with the ones $\vec{p}_0$ that evaluated based on a more representative set of calibration substances. Due to the fact that in the field conditions, the use of a large number of calibration substances makes the calibration process is difficult, the accuracy of RI and NAC retrieval is based on two simplified calibrations set of substances that will be studied further: (a) air and water solution, (b) only air. The method for retrieving the refractive index (RI), $n(f) = Re\sqrt{\varepsilon_s(f)}$, and the normalized attenuation coefficient (NAC), $\kappa(f) = Im\sqrt{\varepsilon_s(f)}$ of samples is based on the iterative method (McCracken et al., 1964) for solving non-linear systems of equation (3)

$$\begin{pmatrix} n_{i+1} \\ \kappa_{i+1} \end{pmatrix} = \begin{pmatrix} n_i \\ \kappa_i \end{pmatrix} + \alpha \left\{ \frac{1}{2k_0 l_s} \begin{pmatrix} arg(F) \\ -ln(F) \end{pmatrix} - \begin{pmatrix} n_i \\ \kappa_i \end{pmatrix} \right\} \qquad (3)$$

where $F = \frac{R + S_{11}^m e^{-2ik_0 l_c}}{1 + R \cdot S_{11}^m e^{-2ik_0 l_c}}$, $R = \frac{Z_c\sqrt{\varepsilon_s} - Z_{s0}}{Z_c\sqrt{\varepsilon_s} + Z_{s0}}$. Choice value of α influences on the convergence rate of the iterative process. The iteration process $0 \leqslant i \leqslant N$ converged approximately for $N = 17$ iterations ($\alpha \equiv 0.7$). It will be noticed that in (3), RI и NAC are the function of the frequency vector of $\vec{f}$. At each i-th step of iteration with using (3), analytically calculates
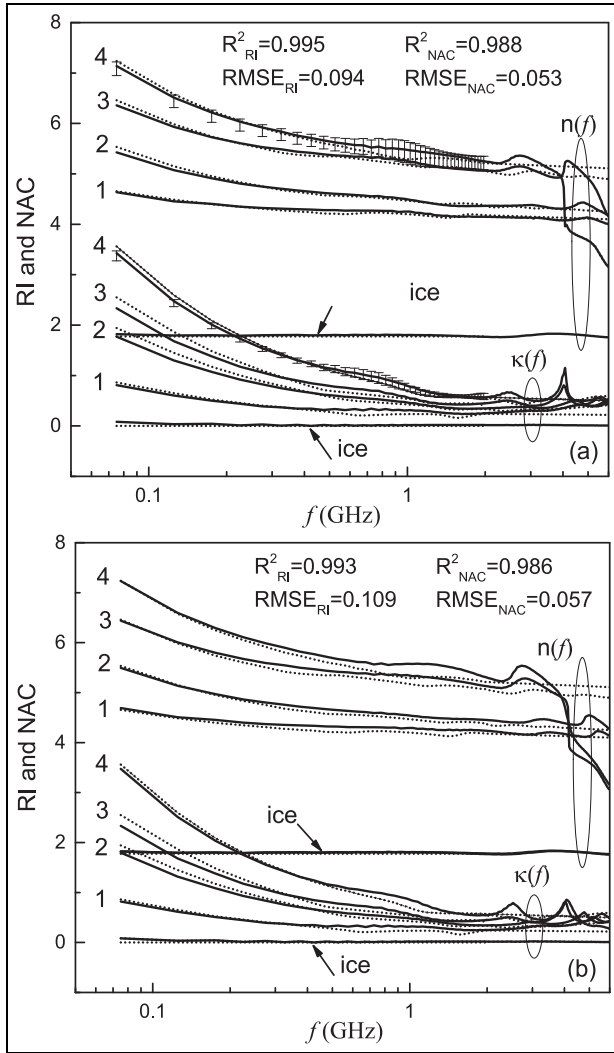
Figure 4. Refractive index (RI) and normalized attenuation coefficient (NAC) measured using: proposed method (solid lines), cylindrical coaxial cell (points).

In the case of ice, dotted lines correspond to the value of ε_s=3.15 + i·0. Soil samples are marked numbers (see Table 1). Results were obtained using the following calibration substances: Panel (a) air and water solution, Panel (b) air only. Statistical estimates were obtained in the frequency range from 75 MHz to 2 GHz.

spectrum of $n_i = n_i(\vec{f})$, $\kappa_i = \kappa_i(\vec{f})$, in the frequency range of $\vec{f} = (f_1, ..., f_{n_f})$, where f_1 and f_{n_f} were taken equal to 75MHz and 6GHz, respectively. To start the iteration process, the values of $n_0 = n_0(\vec{f})$, $\kappa_0 = \kappa_0(\vec{f})$ calculated on the basis (3), with R≡0, n_{-1}≡0, κ_{-1}≡0. Due to a phase change of 2π, a standard unwrapping phase procedure for function F is applied to remove uncertainty.

Discussion

Joint RI and NAC measurements results for the soil specimens with the use of the constructed probe and technique (described in the 'Transmission line model and inverse

method' section) versus precise coaxial cell are depicted in Figure 4. RI, n_{meas}^{cell}, and NAC, κ_{meas}^{cell}, of soils that were measured with the use of the coaxial cell were normalized by a factor, $\rho_d^{cell}/\rho_d^{probe}$, according to the formulas (based on refractive index dielectric model (Mironov et al., 2017)): $n_{norm}^{cell} = n_{meas}^{cell}\rho_d^{cell}/\rho_d^{probe}$, $\kappa_{norm}^{cell} = \kappa_{meas}^{cell}\rho_d^{cell}/\rho_d^{probe}$.

Here, ρ_d^{probe} and ρ_d^{cell} is the dry bulk density of soils samples in plastic cup and in coaxial cell (see Table 1). Such normalization reduces the measurement error of RI and NAC due to differences in the density of samples. The values of RI and NAC were measured by the proposed probe and method using two different sets of calibration substances with a high correlation coefficient $R_{RI,NAC}^2 \approx 0.99$ and small $RMSE_{RI} \approx 0.1$, $RMSE_{NAC} < 0.06$ founds in good agreement (see Figure 4) with respect to measurements in the precision coaxial cell. An error of indirect measurements with the use of the developed technic reaches a maximum value of 0.28 and 0.12 (shown only for soil No. 4, in order not to overload the figure), respectively, for RI and NAC in the region of 0.75-2.0 GHz. These estimates were done based on the formula

$$\Delta g = \sqrt{\sum_{i=1}^{4}\left(\frac{\partial g}{\partial p_i}\Delta p_i\right)^2 + \left(\frac{\partial g}{\partial|S_{11}|}\Delta|S_{11}|\right)^2 + \dots}$$
$$\sqrt{\dots + \left(\frac{\partial g}{\partial argS_{11}}\Delta argS_{11}\right)^2} \quad (4)$$

where $g = n$ or $g = \kappa$. Equation (4) expresses an error estimate of indirect measurements of the function S_{11} calculated on the basis of the error measurement of its arguments, in terms of partial derivatives, similarly as in Baker-Jarvis et al. (2004). In the frequency range above 2GHz, the applicability of the proposed probe and technique is limited by the accuracy of RI and NAC retrieving. In this frequency range, the retrieving error of RI and NAC is due to the straightforward model (1)–(2), limitations of which were described above. In the frequency range of less than 2 GHz, the non-precision probe and the proposed technique can measure the RI and NAC spectra in the field conditions with an accuracy almost comparable to RI and NAC measurements in the laboratory using a precision coaxial cell in the frequaency range from 75 MHz to 2 GHz (see Figure 4). In this case, a simplified calibration can be applied using only one air. The achieved good measurement accuracy is provided by a tight and symmetrical arrangement of the shielding rods close to the coaxial aperture on the SMA connector's flange. The configuration of external shielding rods relative to the central conductor, adjusted during numerical simulation, makes it possible to neglect TM0n modes, which are formed in the transition region of change diameter of SMA connector coaxial line and the outer diameter on which placed the shielding rods. (Taking into account value of a = 1.27 mm and b_e = 7.48 mm, the cutoff frequency for the first TM_{01} mode is $f_{01} \approx$ 3GHz in case of water (Bussey, 1980).) The frequency of 3 GHz is the theoretical maximum operating frequency of the proposed probe.

Conclusion

In contrast to the approaches (Szerement et al., 2019, 2020; Woszczyk et al., 2020, 2019; Wagner, 2011; Wilczek et al.,

2016), the proposed design of the probe allows calculating the reflection coefficient S_{11} used a simple analytical transmission line model (TEM wave mode) rather than calculation with using direct complicated numerical electrodynamic models (FEM, FDTD). The proposed design of a non-precision shielded open-circuited probe is easier to manufacture and provides natural fluxes of moisture and heat in the soil through the measuring area of the probe, in contrast to the sensor proposed in (Lin at al., 2017). The constructed probe based on the standard SMA connector can become a basis for developing a more reliable probe for tough field conditions with various degree of tillage and size of aggregates in natural soil.

Declaration of conflicting interests

The author(s) declared no potential conflicts of interest with respect to the research, authorship, and/or publication of this article.

ORCID iD

Konstantin Muzalevskiy https://orcid.org/0000-0003-2624-7223

References

Baker-Jarvis JR, et al. (2005) Measuring the permittivity and permeability of lossy materials solids, liquids, metals, buildings materials, and negative-index materials. *NIST Technical Note* 1536, p. 172.

Bircher S,, et al. (2016) Soil moisture sensor calibration for organic soil surface layers. *Geos. Instr. Meth. and Data System* 5: 109–125.

Buckley F and Maryott AA (1958) Tables of dielectric dispersion data for pure liquids and dilute solutions. Washington, D. C.: U.S. Dept. of Comerce, *National Bureau of Standards*. 95 p.

Bussey HE (1980) Dielectric measurements in a shielded open circuit coaxial line. *IEEE Transactions on Instrumentation and Measurement* 29(2): 120–124.

Demontoux F, Razafindratsima S, Bircher S, et al. (2017) Efficiency of end effect probes for in-situ permittivity measurements in the 0.5–6 GHz frequency range and their application for organic soil horizons study. *Sensors and Actuators, A: Physical* 254: 78–88.

Du J, Kimball JS and Moghaddam M (2015) Theoretical modeling and analysis of L- and P-band radar backscatter sensitivity to soil active layer dielectric variations. *Remote Sensing* 7: 9450–9472.

Guihard V, Taillade F, Balayssac JP, et al. (2019) Permittivity measurement of cementitious materials and constituents with an open-ended coaxial probe: Combination of experimental data, numerical modelling and a capacitive model. *RILEM Technical Letters* 4: 39–48.

Guihard V, Taillade F, Balayssac JP, et al. (2020) Permittivity measurement of cementitious materials with an open-ended coaxial probe. *Construction and Building Materials* 230: 116946.

Heimovaara TJ (1994) Frequency domain analysis of time domain reflectometry waveforms 1. Measurement of the complex dielectric permittivity of soils. *Water Resources Research* 30(2): 189–199.

Heimovaara TJ, et al. (1996) Frequency-dependent dielectric permittivity from 0 to 1 GHz: Time domain reflectometry measurements compared with frequency domain network analyzer measurements. *Water Resources Research* 32(12): 3603–3610.

Jackisch C, Germer K, Graeff T, et al. (2020) Soil moisture and matric potential – An open field comparison of sensor systems. *Earth Syst. Sci. Data* 12: 683–697.

Komarov SA, Komarov AS, Barber DG, et al. (2016) Open-ended coaxial probe technique for dielectric spectroscopy of artificially grown sea ice. *IEEE Transactions on Geoscience and Remote Sensing* 54(8): 4941–4951.

Lemmetyinen J, Schwank, M, Rautiainen K, Kontu A, Parkkinen T, Mätzler C, Wiesmann A, Wegmüller U, Derksen C, Toose P, Roy A, Pulliainen J. (2016) Snow density and ground permittivity retrieved from L-band radiometry: Application to experimental data. *Remote Sensing of Environment* 180: 377–391.

Lin CP, et al. (2017) A novel TDR signal processing technique for measuring apparent dielectric spectrum. *Meas. Sci. Technol.* 28: 015501.

McCracken DD, et al. (1964) *Numerical Methods and Fortran Programming with Applications in Engineering and Science*. New York: John Wiley & Sons.

Majcher J, Kafarski M, Wilczek A, et al. (2020) Application of a monopole antenna probe with an optimized flange diameter for TDR soil moisture measurement. *Sensors* 20(8): 2374.

Mavrovic A, Madore JB, Langlois A, et al. (2020) Snow liquid water content measurement using an open-ended coaxial probe (OECP). *Cold Regions Science and Technology* 171: 102958.

Mavrovic A, Pardo Lara R, Berg A, et al. (2021) Soil dielectric characterization during freeze–thaw transitions using L-band coaxial and soil moisture probes. *Hydrol. Earth Syst. Sci.* 25: 1117–1131.

Mavrovic A, Roy A, Royer A, et al. (2018) Dielectric characterization of vegetation at L band using an open-ended coaxial probe. *Geosci. Instrum. Method. Data Syst.* 7: 195–208.

Mironov VL, et al. (2017) Temperature- and texture-dependent dielectric model for frozen and thawed mineral soils at a frequency of 1.4 GHz. *Remote Sensing of Environment* 200: 240–249.

Robinson DA, et al. (2003) A review of advances in dielectric and electrical conductivity measurement in soils using time domain reflectometry. *Vadose Zone Journal.* 2(4): 444–475.

Stogryn A (1971) Equations for calculating the dielectric constant of saline water (correspondence). *IEEE Transactions on Microwave Theory and Techniques* 19(8): 733–736.

Szypłowska A, et al. (2016) Soil complex dielectric permittivity spectra determination using electrical signal reflections in probes of various lengths. *Vadose Zone Journal* 15(3): 1–12.

Szerement J,, et al. (2019) A seven-rod dielectric sensor for determination of soil moisture in well-defined sample volumes. *Sensors* 19: 1646.

Szerement J,, et al. (2020) Dielectric properties of glass beads with talc as a reference material for calibration and verification of dielectric methods and devices for measuring soil moisture. *Materials* 13(8): 1968.

Xu J,, et al. (2012) Short, multineedle frequency domain reflectometry sensor suitable for measuring soil water content. *Soil Sci. Soc. Am. J.* 76(6): 1929–1937.

Wagner N (2011) On the coupled hydraulic and dielectric material properties of soils: combined numerical and experimental investigations. In: *9th International Conference on Electromagnetic Wave Interaction with Water and Moist Substances*, USA, Kansas City, 31 May–3 June 2011, pp. 152–161.

Wilczek A, et al. (2016) Time-domain reflectometry method with variable needle pulse width for measuring the dielectric properties of materials. *Sensors* 16(2): 191.

Woszczyk A, Szerement J, Lewandowski A, et al. (2019) An open-ended probe with an antenna for the measurement of the water content in the soil. *Computers and Electronics in Agriculture* 167: 105042.

Woszczyk A, et al. (2020) A modified open-ended probe as a reliable tool for measurements of soil water content. In: *Baltic URSI Symposium (URSI)*, Warsaw, Poland, 5-8 Oct. 2020, pp. 161–164.